Chapter 10

BiOX (X = Cl, Br, and I) Photocatalysts

Liqun Ye

Additional information is available at the end of the chapter

http://dx.doi.org/10.5772/62626

Abstract

Photocatalysis technology has been wildly used to remove the most pollutants for environmental remediation under light irradiation. This chapter summarized the applications of BiOX (X = Cl, Br, and I) photocatalysts, including synthesis, photocatalytic performance without modification, enhanced VLD photocatalytic activity with the modification, and photocatalytic stability. Photocatalytic degradation (PCD) removal of volatile organic compounds (VOCs), contaminated chemicals, organic pollutants, and biological substances were introduced in this chapter. On the other hand, the morphologies, bismuth-rich effects, facet effects, and photocatalytic mechanisms of BiOX were discussed to provide effective methods for designing highly visible-light-driven (VLD) photocatalytic activity BiOX photocatalysts. The unsatisfactory points and future research directions also were briefly discussed at the end.

Keywords: BiOX, photocatalysis, environmental, bismuth-rich, facet effect

1. Introduction

Twenty-first century, with the urbanization and the industrialization increasing dramatically, the contamination caused by solid waste, gases, contaminated chemicals, organic pollutants, and biological substances has become a severe problem [1–3]. At present, many organic pollutants are in very low concentration and are high toxic. Therefore, it is required an effective and "green" method to transform them into non-hazardous compounds without secondary pollution [4–6]. In the past years, physical treatment methods (adsorption, ultrafiltration, coagulation, etc.) and chemical degradation methods (include ozone/UV radiation/H_2O_2 oxidation, semiconductor photocatalysis technique, advanced oxidation, photo-fenton reaction, and photo-electrochemical method) were the main ways to eliminate the environmental contaminants [7, 8]. Among the above methods, semiconductor photocatalysis technique can

degrade the contaminants completely, environmental friendly, rapidly, and cheaply. It has been suggested as one of the most effective and "green" ways to eliminate the environmental contaminants [9–12].

Photocatalyst is the body of photocatalysis technique. Therefore, the development of high-performance photocatalysts has attracted great interest. To date, there are two main synthesis strategies that have been investigated for the preparation of high-activity photocatalysts. The first one is to extend the modification of conventional photocatalysts (simple oxides, sulfides) by doping, coupling, and sensitization. The other strategy is to develop new photocatalysts. The former has been obtained many achievements, but it still cannot satisfy the requirement for practical application. So, more and more researchers changed to explore new high-efficiency photocatalysts, such as complex oxides, AgX (X = Cl, Br, I), and polymer [13–17]. BiOX (X = Cl, Br, I) are important V–VI–VII ternary semiconductor compounds because of their optical properties. All BiOX are tetragonal matlockite structure with $[Bi_2O_2]$ slabs interleaved by double halogen atom slabs (**Figure 1**). In the past reports, BiOX were usually applied as thermal-induced catalysts [18, 19], ferroelectric materials [20], energy storage materials [21], and pigments [22]. Recently, BiOX were reported as photocatalysts to degrade pollutants for environmental remediation and solar fuel production. And more and more workers study the photocatalytic performance of BiOX under sunlight irradiation.

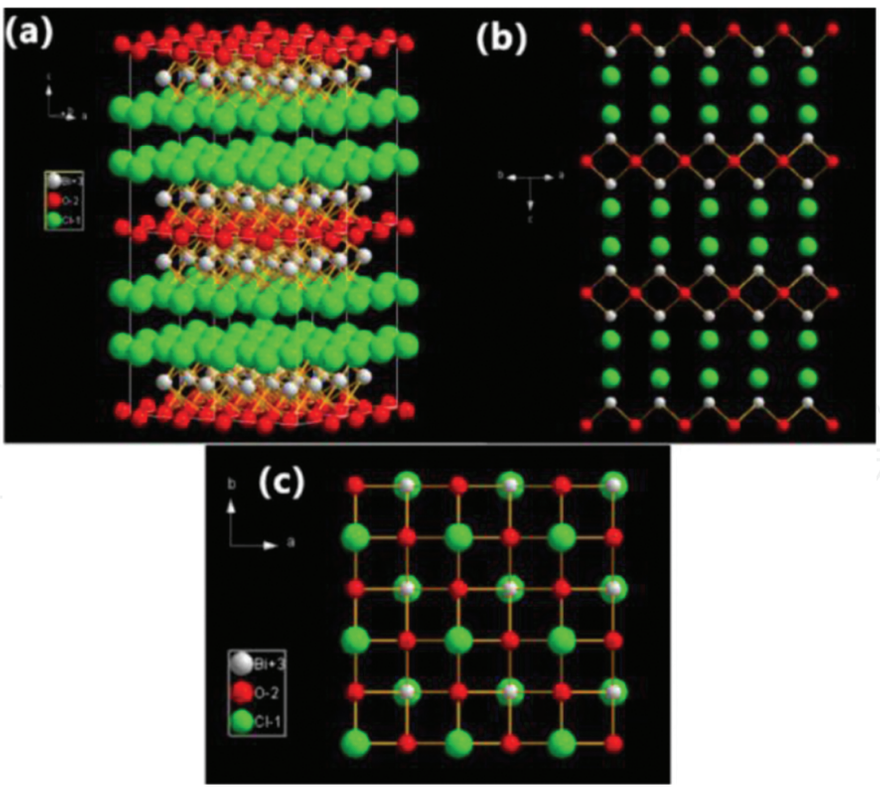

Figure 1 The 3 × 3 lattices model of BiOCl crystals (3 × 3 lattices): (a) three-dimensional projection; (b) [110] direction; and (c) [001] direction.

Structure determines the features. For BiOX, their open crystalline structure resulted the outstanding photocatalytic activity. The open-layered structure means enough space to polarize the related atoms and orbitals and then to induce the presence of internal static electric fields which are perpendicular to {001} facets of BiOX [23–28]. On the other hand, it has reported that the excited electron should travel a certain k-space distance to be emitted to the valence band (VB) due to the indirect-transition bandgap [23–28]. Therefore, BiOX displayed low recombination probability of the excited electrons and the holes, and the outstanding photocatalytic activity was obtained. Among BiOCl, BiOBr, and BiOI, BiOCl exhibited the best UV light–induced photocatalytic activity and even displayed higher activity than TiO_2 (P25, Degussa) for photocatalytic degradation (PCD) of dyes. BiOI exhibited the best photocatalytic activity for PCD of organic pollutants under the visible light irradiation attributed to its smallest bandgap. BiOBr has the appropriate bandgap (2.7–2.9 eV), which results in the best photocatalytic activity under full light spectrum irradiation.

In this chapter, we summarize the recent advances on BiOX. It may give us insight into the trend in the development of BiOX for environmental protection. At present, PCD of gas-phase and liquid-phase substrates over BiOX are researched widely. But PCD of solid-phase substrates was researched very few due to the long research cycle [29–33]. For example, all organic compounds, bacteria and heavy metals can be removed by BiOX via liquid-phase photocatalysis under light irradiation. VOCs and NO_x can be decomposed by BiOX via gas-phase photocatalysis. Polyvinyl chloride (PVC) can be decomposed by BiOI via solid-phase photocatalysis [29]. The detailed pollutant degradation pathways and the intermediates of mainly pollutants also were shown. In addition, we also emphasize on the modification, facet effect, bismuth-rich effect, and the photocatalytic mechanisms of BiOX for efficient photocatalytic applications in this review, which can provide effective methods develop much higher photocatalytic activity BiOX photocatalysts for environment photocatalysis. At end, the unsatisfactory points and future research directions are simply discussed.

2. Synthesis

2.1. Methods

The size, surface area, and morphology of photocatalysts can be changed with different synthesis method using. And the cheap and "green" methods were also necessary for the industrialized applications [34–37]. The bismuth sources include $Bi(NO_3)_3 \bullet 5H_2O$, $NaBiO_3 \bullet 2H_2O$, Bi_2O_3, Bi, $BiCl_3$, and BiI_3. And CTAX (X = Cl, Br, or I) KX (X = Cl, Br, or I), NaX (X = Cl, Br, or I), HX (X = Cl, Br, or I), and ionic liquid with halogen element were usually used as halogen source [38–66]. At present, the main BiOX synthesis methods included precipitation, solvothermal, reverse microemulsions route, molecular precursor route, calcination, microwave irradiation process, ionic liquid modified, etc. Furthermore, the pH value, reaction temperature, and reaction time also can affect the synthesis of BiOX.

The reported morphology indicated that BiOX were single-crystal nanosheets or 3D hierarchical structures with nanosheets. In addition, BiOI quantum dot was reported by Liu [42]. The

size of BiOI quantum dot can be controlled <5 nm. As-synthesized RGO/BiOI nanocomposites showed very high photocatalytic activity under visible light irradiation. Except for BiOX quantum dot, one-dimension nanobelts also was synthesized with reaction temperature at 160–180°C and pH value at 8. But the exposed dominant facet of BiOX nanobelts also were {001} facet which is in agreement with two dimension BiOCl nanosheet [67]. It is indicated that BiOX generally exposed {001} facets, and the synthesis methods cannot change the dominant facet easily.

2.2. Synthesis mechanisms

Synthesis mechanisms were the key roles to suggest us perfecting the synthesis factors. For BiOX, the main-based morphology was 2D nanosheets. In liquid reaction, the formation of 2D structure was due to the low surface energy of {001} facets and layer structure of BiOX. In solid reaction, the BiOX 2D structure can be obtained via chemical transport. For example, our group synthesized BiOI nanosheets with very high symmetry with thermal treatment of BiI_3 [60]. **Figure 2** showed the possible synthesis mechanisms. BiI_3 reacted with O_2 to produce BiOI and iodine vapor when the temperature higher than 350°C. At the same time, BiI_3 also can be sublimated. The freed off iodine and BiI_3 vapors spilling over from bulk BiI_3, the pressure resulted the BiOI nanosheets shelling from BiI_3.

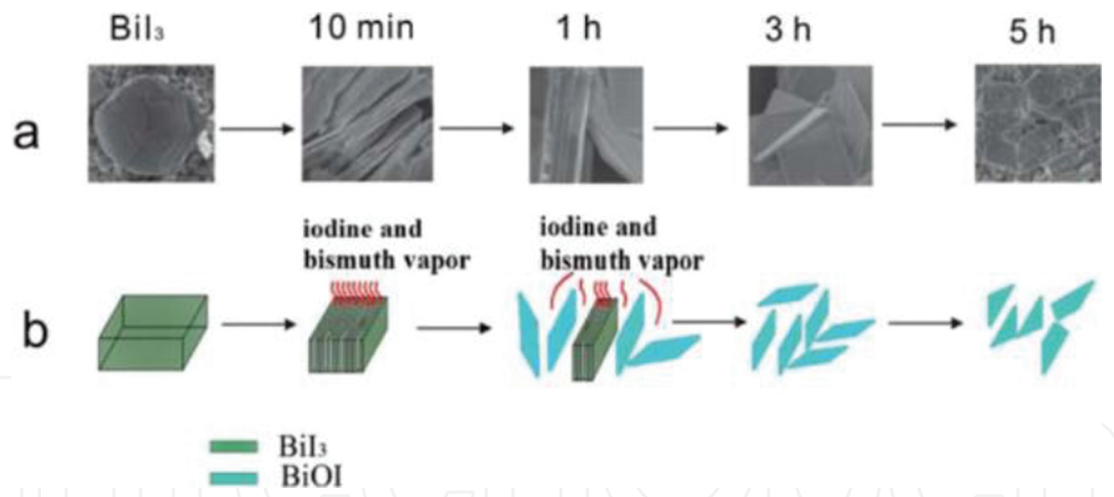

Figure. 2 Illustration of formation mechanism of BiOI SCNs: (a) original formation process; (b) simulation formation process [60]. Reprinted with permission from Royal Society of Chemistry.

3. Photocatalytic performance of pure BiOX

3.1. Photocatalytic activity

Since Huang reported BiOCl for photocatalytic dye degradation at 2006 [23], BiOX were widely studied as photocatalysts. In general, BiOCl displayed high photocatalytic activity for dyes (RhB, MO, MB, etc.) and phenols degradation under UV, visible, or UV–Vis light irradiation

via excitation of BiOCl or dye sensitization pathway [68]. BiOI can absorb more visible light (ca. 650 nm) than BiOCl (ca. 360 nm) and BiOBr (ca. 430 nm). Therefore, BiOI showed higher photocatalytic activity than BiOCl and BiOBr under visible light irradiation. For example, Zhang reported that the BiOI displayed higher photocatalytic activity than BiOBr and BiOCl for methyl orange degradation [38]. Lei synthesized BiOI flower-like hierarchical structures with higher photocatalytic activities for dyes and phenol degradation under visible light irradiation than the BiOI platelets [59]. Due to the most appropriate bandgap (2.8 eV), BiOBr showed the best photocatalytic oxidation and reduction activity under full light spectrum irradiation. So, it can be used to remove more organic pollutants, especially for bacterium and microcystin-LR [49–53, 69–71]. Until now, only BiOBr usually was reported to photo-degrade biological substances. For instances, Yu found that hierarchical BiOBr microspheres can effectively kill Micrococcus lylae, a positive bacterium, in water under fluorescent light irradiation [50]. Wong also reported the facets effect of BiOBr for *Escherichia coli* photocatalytic inactivation [70]. Fang firstly reported Microcystin-LR degradation over BiOBr under visible light irradiation [71].

3.2. Photocatalytic selectivity

Catalytic data included many parts, and selectivity was a very important factor. In TiO_2 system, selective photocatalytic degradation of alcohols and azo dyes has been paid more attention [72–76]. However, TiO_2 without surface modification showed very poor photocatalytic selectivity due to the low adsorption selectivity. In order to obtaining high photocatalytic selectivity, TiO_2 was usually modified by surfactant to enhance the adsorption selectivity. For BiOX system, the atoms structural (**Figure 1**) showed that the dominant {001} facets of BiOX covered with 100% terminal oxygen atoms. So, {001} facets of BiOX should be more negatively charged than other facets. And, BiOX nanosheets with dominant exposed {001} facets can show very high adsorption selectivity for cationic dyes and result in high photocatalytic degradation selectivity.

Recently, our group reported the photocatalytic selectivity of BiOI. By analyzing the UV–Vis absorption spectra during the photocatalytic degradation of RhB with BiOI, we found that the characteristic absorption peak of RhB exhibited obvious blue shift (from 554 to 500 nm). This phenomenon indicated that the mainly PCD path of the RhB was deacetylation process. On the other hand, once RhB molecules were adsorbed on the surface of BiOI, a new N1s XPS peak appeared at 401.1 eV, and the shift was about 1.8 eV compare to the pure RhB due to the interaction between the {001} facets of BiOI and the N^+ group of RhB. So, it can be suggested that adsorption selectivity of BiOI for RhB and resulted in high photocatalytic degradation selectivity. Furthermore, the photocatalytic results showed that the degradation rates of MB were much faster than those of MO for BiOI TF, and the selective photocatalytic ability R ($R = k_{MB}/k_{MO}$) is 6.9 which are six times higher than TiO_2 TF. It implied that BiOI displayed high selective photocatalysis.

3.3. Photocatalytic stability

Except for photocatalytic selectivity, photocatalytic stability was another important factor for the practical application. It has been reported that the affect factors of photocatalytic stability included intrinsic structure and solubility product constant of photocatalyst, pH value, and properties of substrate. As g-C_3N_4, the interaction force between layers of BiOX also was van der Waals force, but covalently bonded layers also appeared in BiOX layer structure. So, BiOX are more stable than other layer photocatalysts such as g-C_3N_4 whose interaction force between layers is van der Waals force. It had been reported that the solubility product constant of BiOCl is very low with 1.8×10^{-31}, which indicated that BiOX cannot easily dissolve or transform under normal circumstances. However, the pH value and properties of substrate can affect the stability of BiOX. For example, BiOX can dissolve under acid environment [68] and can react with S_2^- to transform to Bi_2S_3 [66].

For BiOCl, Huang firstly evaluated the photocatalytic stability of BiOCl [28]. The stable XRD pattern and cycles reaction of BiOCl revealed the stability for the PCD of dyes, and this conclusion was also proved by Sarwan [68]. For BiOBr, Huo researched the photocatalytic stability by comparing the photocatalytic activity, crystallization and morphology after six photocatalytic cycles [69]. The photocatalytic stability of BiOI also was proved as stability VLD photocatalyst by our group and Zhang' group [59]. However, the photocorrosion of BiOX was not considered. The releasing traces of Bi via photocorrosion of BiOX are critical for environment. So, in future work, the photocorrosion of BiOX should be taken into account.

3.4. Degradation pathways and intermediates of pollutant over BiOX

In reported works, the main study of BiOX photocatalysts focuses on enhancing the photocatalytic activity for environmental remediation. But the degradation pathways of pollutant were researched very few. For gas-phase substrate photocatalytic degradation, Zhang reported the degradation pathways and intermediates of NO [54]. The amount of NO_3^- increased with prolonged illumination, but the amount of NO_2^- kept almost constant at 0.08 μmol with reaction time. It implied that NO to NO_3^- was the major the oxidation pathway for NO over BiOBr microspheres. Furthermore, it had been reported that the NO_3^- and NO_2^- came from the reaction between NO_x and $O_2^{\bullet-}$ and •OH, respectively. Therefore, $O_2^{\bullet-}$ was the major reactive oxygen species (ROS) for NO remove over BiOBr.

For liquid-phase substrate photocatalytic degradation, dyes (such as MO, MB, and RhB) and phenols were the most used substrates. The degradation pathways and intermediates of dye molecules had been studied deeply. So, in this chapter, we did not discuss it. On the contrary, the degradation pathways of phenols were complex, and it is meaningful to investigate the degradation pathways and intermediates of phenols. In BiOX/UV–Vis systems, Chen [76] proved that hydroxyl adducts such as catechol and hydroquinone were the main intermediates for phenol degradation. Meng showed that the degradation of tetrabromobisphenol A started with hydroxylation and debromination. As shown in **Figure 3**, •OH was the major reactive oxygen species [51].

http://dx.doi.org/10.5772/62626

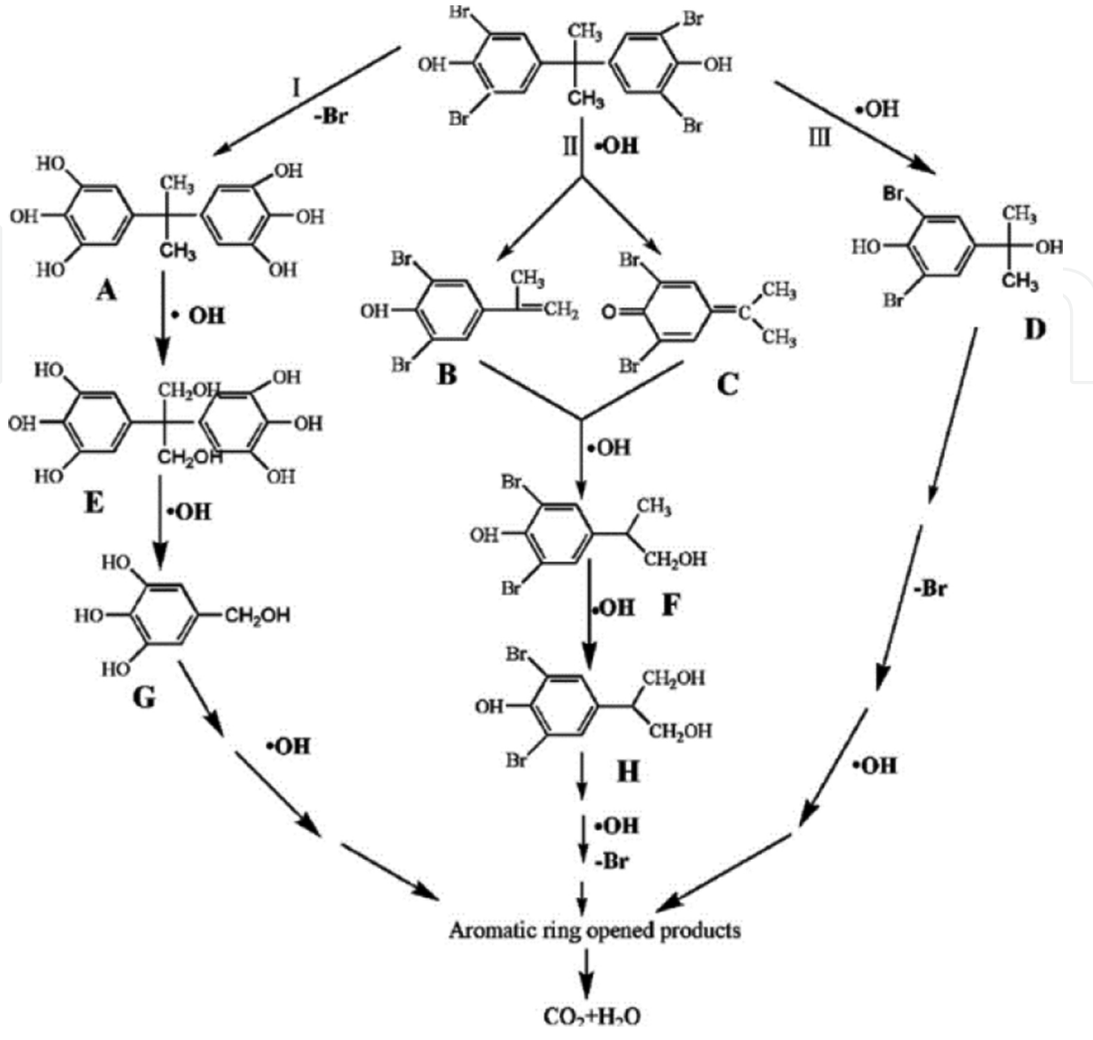

Figure. 3 Proposed TBBPA degradation pathway [51]. Reprinted with permission from Elsevier.

In addition, microcystins-LR is a very hazardous pollutant. It can cause sickness in life body, and World Health Organization has identified it as strongly hepatotoxic. Recently, Huang reported the degradation pathways and intermediates of microcystins-LR in BiOBr/vis systems [70]. Isotope labeling technique proved the decarboxylation process over BiOBr. Furthermore, •OH and hole were the active species for MC-LR remove.

4. Modification for enhanced VLD photocatalytic activity

In general, there are three key steps (light harvesting, photo-induced carriers separation, and the photocatalytic reduction and oxidation reactions) for photocatalytic processes. At present, although BiOX had excellent photocatalytic activity for environmental contaminants degradation, the photocatalytic activity of BiOX were still very low and cannot be used for practical application under sunlight irradiation. For improving the VLD photocatalytic activity of BiOX, many modification strategies had been applied to enhance the solar light harvesting and photo-

induced carriers separation. These strategies included cocatalyst using, element doping, semiconductor coupling, dye sensitization, surface plasmon resonance, defect making, bismuth-rich effect, and so on [77–150]. And the above methods successfully improved the VLD photocatalytic activity of BiOX.

4.1. Cocatalyst

Cocatalysts of photocatalysts can act as reaction sites and active sites. It also provided photogenerated charges trapping sites to promote the photo-induced carriers separation. Then, enhanced photocatalytic activity was displayed [82, 152]. Therefore, at presently, cocatalyst wildly used to enhance the photocatalytic activity of photocatalysts for environmental pollutants degradation and solar fuels generation. Recently, cocatalysts were divided into deriving-electron types (Ag, Pt, Au) and deriving-hole-types (PbO_2, MnO_x) [82, 152]. Our group reported that deriving-hole types cocatalyst (MnO_x) enhanced the separation efficiency of the photo-induced carriers better than that of deriving-electron types (Pt) over BiOI, and then improve the photocatalytic activity for PCD of dye (**Figure 4**) [78–81]. Analyzing the reason, it must be pointed out that almost all of works suggested holes as the main active species over BiOX photocatalysts for degrading pollutants. Therefore, deriving-hole-type cocatalysts showed more effective for enhancing the photocatalytic activity of BiOX.

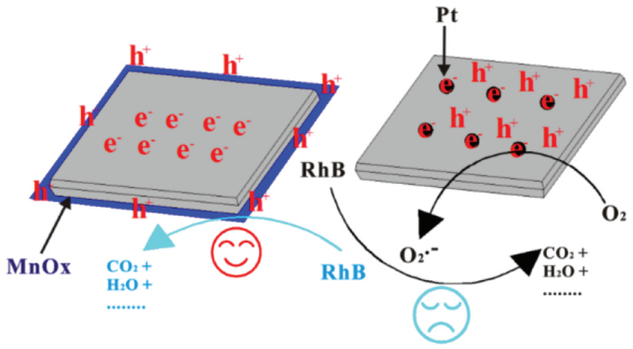

Figure 4 The mechanism of cocatalyst selectivity of BiOI under visible light irradiation ($\lambda \geq 420$ nm) [82]. Reprinted with permission from Royal Society of Chemistry.

4.2. Element doping

Element doping had been wildly used to enhance the photocatalytic activity in TiO_2 system. The defect energy level decreased bandgap enhanced visible light harvesting and defect sites improved trapping of electrons to inhibit electron–hole recombination. Recently, it has been reported that C, I, N, and Mn-doped BiOCl with an obvious red shift compared to the pure BiOCl and resulted in excellent photocatalytic activity under visible light [84–87]. It indicated that the element doping can effectively expand the light adsorption region. In order to surface photovoltage spectroscopy (SPS) and transient photovoltage (TPV), measurements were used to prove the visible light harvesting ability and separate efficiency of photo-induced electron–hole of self-doping BiOX. The increased SPS signal intensity implied that the generation of

electron–hole pairs can be enhanced on $BiOI_{1.5}$due to its good visible light harvesting ability. The increased TPV signal intensity indicated that the photo-induced electron–hole pairs of $BiOI_{1.5}$ were separated more easily than that of BiOI. Therefore, self-doping $BiOI_{1.5}$ displayed higher VLD photocatalytic activity than pure BiOI [83]. On the other hand, the facets-dependent C-doping mechanism of BiOCl also was studied as shown in **Figure 5**. The impurity energy level of carbon caused the absorption edge shifting to higher wavelength and increasing the lifetime of charge carries. Thus, the photocatalytic activity of BiOCl was enhanced by both the effective usage of light source and the inhibition of recombination of photo-induced charge carriers [85].

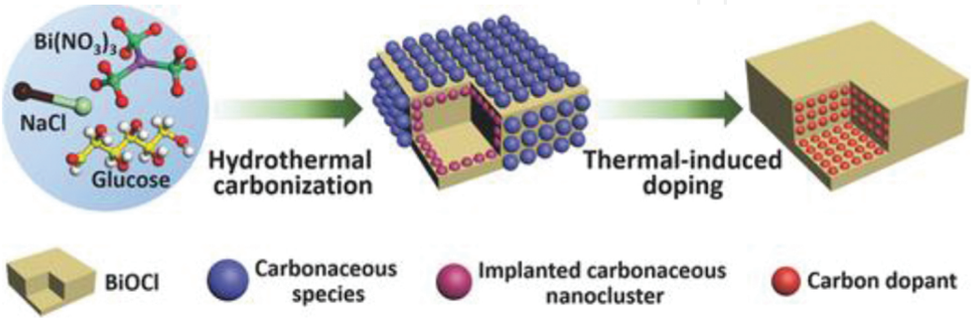

Figure 5 Schematic illustration of homogeneous carbon doping strategy comprised of bottom-up hydrothermal processing and subsequent thermal treatment with taking carbon doped BiOCl as the example [85]. Reprinted with permission from Wiley.

4.3. Semiconductor coupling

Semiconductor coupling photocatalysts constructed a heterojunction interface between two type semiconductor photocatalysts with matching energy bandgaps. It has been becoming the most important method to enhance the photocatalytic efficiency by improving the photo-induced carriers separation and expanding the energy range of photoexcitation for the system, thus achieving better photocatalytic activity for dye degradation. In generally, two photocatalysts coupling do not show selectivity [90–130]. In our recent work, we found that the interaction between BiOBr and g-C_3N_4 was facet (2D/2D) coupling between BiOBr-{001} and g-C_3N_4-{002}. The facets coupling resulted in photo-induced charges transfer between BiOBr and g-C_3N_4 and improve the VLD photocatalytic activity for environmental remediation. This research offered a possible explanation for the 2D/2D heterojunction of inorganic–organic composite photocatalysts [103].

4.4. Graphene

Because graphene's superior physical and chemical properties, it has stimulated great interests for preparing many functional composite materials with outstanding applications [20]. For BiOX photocatalysts, modification with graphene also was researched strongly. Our group and Zeng's group suggested the C–Bi chemical coupling improved photo-induced charges separation [131, 132]. Based on this advantage, graphene-BiOCl exhibited enhanced photoca-

talytic activity. The similar photocatalytic results of graphene-BiOBr also were reported by Li, Zhang, Ai, and Bai [133–136]. They proved that the enhanced photocatalytic activity come from the strong C–Bi chemical bonding, rather than their higher surface area and light absorption extension in the visible region between BiOBr and graphene. For graphene-BiOI, RGO/BiOI nanocomposites showed improved photocatalytic activity for dye degradation under visible light. But C–Bi chemical coupling did not found in graphene-BiOI system, and Fang suggested that the improved light absorption and efficient charge separation and transportation induced the improved photocatalytic activity under visible light irradiation [42].

4.5. Dye sensitization

Chemisorbed or physisorbed photosensitizers (dye molecules or quantum dots) can expand the spectrum range from UV light to the full spectrum. The excited-state electrons of sensitizer can transfer to the photocatalysts, and then the photocatalysis reaction occurred at the conduction band (CB) of photocatalysts. Organometallic complex were the most using sensitizers Copper complexes, ruthenium complexes (N719, C101, C102, and $[Ru(bpy)_3]^{2+}$), and zinc complexes were all used as photosensitizers [153–157]. For example, simultaneous over all water splitting and RhB degradation reaction occurred on copper phthalocyanine (CuPc) sensitized BiOCl composite under simulated solar light irradiation [150]. However, we known that ruthenium complexes are difficult to synthesize and very expensive. Copper and zinc complexes displayed very low efficiencies. So, it is very important to develop some new sensitizers.

In our recent work, $Bi_n(Tu)_xCl_{3n}$ bismuth complexes were used as new sensitizers. $Bi_n(Tu)_xCl_{3n}$ inner sensitized BiOCl displayed very high photocatalytic activity under visible light ($\lambda > 420$ nm) (**Figure 6**) [150]. At present, there were few reports about inner sensitized photocatalysts system. Most photosensitizers were absorbed on the surface of photocatalysts. Obviously, the inner sensitization displayed many advantages. Firstly, the stability of inner sensitized photocatalysts system was enhanced. This sensitized type avoided the sensitizer consumption during the photocatalytic process. Secondly, it expanded the applied condition of the sensitizers. For example, water soluble photosensitizers can be used in the in-aqueous solution by inner sensitization.

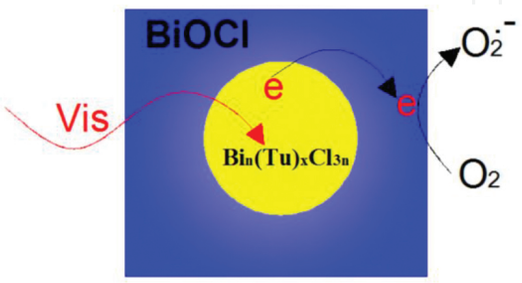

Figure 6 $Bi_n(Tu)_xCl_{3n}$ sensitized the BiOCl and resulted in unusual high visible light pholocatalytic activity [150]. Reprinted with permission from Royal Society of Chemistry.

4.6. Surface plasmon resonance

Surface plasmon resonance (SPR) can be improved the visible light absorption dramatically and offered new way to develop new VLD photocatalysts. Among noble metals, Ag was suggested as the best SPR effects. Therefore, more interests have been paid to Ag–TiO_2, Ag–ZnO, Ag/AgX (X = Cl, Br, I), Ag/$AgPO_4$, Ag/AgBr/TiO_2, Ag/AgBr/Bi_2WO_6, and Ag/AgBr/WO_3 three composite photocatalysts to enhance the VLD photocatalytic activities [162–173]. For BiOX system, Ag/AgCl/BiOCl and Ag/AgBr/BiOBr showed much higher VLD photocatalytic activity for pollutants degradation than Ag/AgX and pure BiOX [137–144]. Furthermore, superoxide radical quantification and active species trapping experiments showed that metallic Ag played different role for Ag/AgX/BiOX VLD photocatalysts. SPR for Ag/AgCl/BiOCl, and the Z-scheme bridge for Ag/AgBr/BiOBr [144]. As shown in **Figure 7**, the photo-induced electrons transferred from metallic Ag to the CB of AgCl and further transferred to the CB of BiOCl. Then, the electrons reacted with O_2 to produce $O_2^{\bullet-}$ for RhB degradation. And the photogenerated holes transfer to the VB of AgCl and BiOCl to oxidize Cl^- ions with Cl· radicals producing. The Cl radical can degrade RhB, and hence, Cl·was reduced to Cl^- ions again [144]. Based on the photocatalytic mechanism analysis, we deemed that metallic Ag had very important role in SPR.

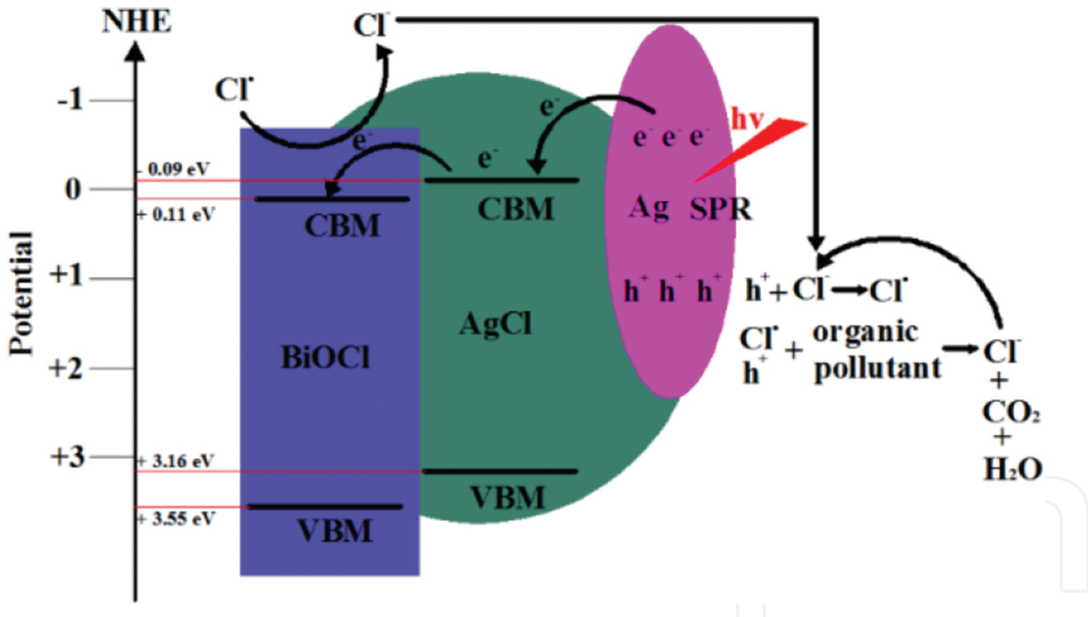

Figure 7 Photocatalytic mechanism scheme of Ag/AgCl/BiOCl under visible light irradiation ($\lambda \geq 400$ nm) [144]. Reprinted with permission from American Chemical Society.

4.7. Defects

In previous reports, it had been proved that the oxygen vacancies occurred under UV light irradiation due to the low-bond energy and long-bond length of the Bi–O bond [47]. Furthermore, our group prepared black BiOCl with oxygen vacancies 20 times higher VLD photocatalytic activity than pure BiOCl for RhB degradation [148]. Recently, Xie found the defects

change from isolated defects V_{Bi}''' to triple vacancy associates $V_{Bi}'''V_O^{\bullet\bullet}V_{Bi}'''$ with the thickness of BiOCl nanosheets reducing to 3 nm [149]. And the ultrathin BiOCl nanosheets showed five times higher VLD photocatalytic activity than bulk BiOCl nanoplates (30 nm) for RhB degradation.

4.8. Solid solutions

It has been reported that the absorption edges of $BiOCl_{(1-x)}Br_x$, $BiOBr_{(1-x)}I_x$, and $BiOCl_{(1-x)}I_x$ solid solutions changed as a function of x, and they all displayed enhanced VLD photocatalytic activities than pure BiOX [145–147]. The reasons of the good VLD photocatalytic activity of BiOX solid solutions may be the enhanced internal electric field and the deeply valence band edge position [146, 147]. Alternatively, by DFT calculations, Huang considered that the trapping of photogenerated carriers in BiOX solid solutions arises the most likely from the cation vacancy V_{Bi} [145].

4.9. Bismuth-rich effect

BiOX photocatalyst also has its drawbacks. The conduction band positions of BiOX are too positive, limiting its ability of activating molecular oxygen, degradation of pollutants, and other applications. For improving its photocatalytic activity, the CB position must be decreased. It has been proved that the CB of bismuth-based photocatalyst mainly included Bi 6p orbits. Therefore, the increase bismuth content may decrease the CB potential, and then, the bismuth-rich $Bi_xO_yX_z$ (X = Cl, Br, I) showed very high photocatalytic reduction activity. For example, Huang found that the increments of the content of bismuth in bismuth titanate can improve the position of CBM [178]. Since Huang' group first reported Bi_3O_4Cl photocatalyst in 2006 [179], several other $Bi_xO_yX_z$ photocatalysts such as Bi_3O_4Cl, Bi_3O_4Br, $Bi_4O_5I_2$, $Bi_4O_5Br_2$, $Bi_{24}O_{31}Cl_{10}$, $Bi_{24}O_{31}Br_{10}$, Bi_5O_7I, Bi_5O_7Br, $Bi_7O_9I_3$ were reported and showed higher activity than their corresponding BiOX [179–190].

5. Facet effect

Different crystal surface of nanomaterials showed different electronic and geometric structures and also exhibited different surface physical, chemical properties, and photoreactivity. Therefore, the facet-dependent photocatalytic properties have aroused much research interest [191–197]. Since Yang firstly reported {001} facet-dependent photocatalytic properties of anatase TiO_2 properties [198, 199], anatase TiO_2 has been intensively investigated with different facet exposure [200–217]. Except for TiO_2, the facet-dependent photocatalytic properties of many other photocatalysts, such as ZnO [219–221], $BiVO_4$ [152, 194], AgBr [195], and $AgPO_4$ [197, 222], also were studied. For BiOX, the layer structure resulted that the mainly exposed facets were {001}, and other facets ({100} or {010} facets) of BiOX were very difficult to expose. So, until 2011, the facet-dependent photocatalytic properties of BiOX were reported by our group for the first time. Our group and Zhang's group have detailedly researched the facets effect of BiOCl [44, 60, 223, 224]. And then, the facets effects of BiOBr and BiOI were reported

[225–228]. But, the relevant studies about facet-dependent photocatalytic properties of BiOX were still very limited.

5.1. {001} facet

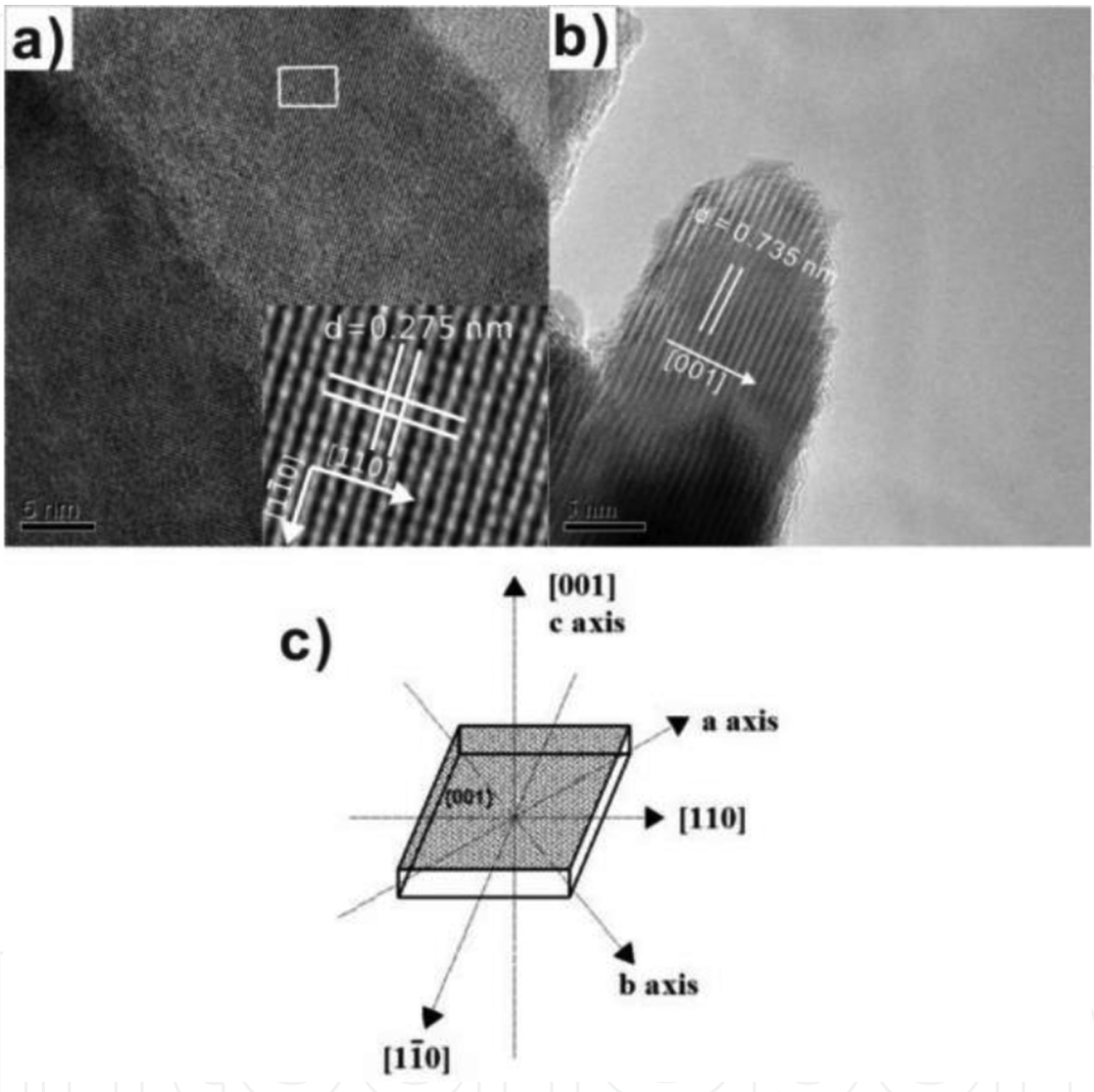

Figure 8 (a) Top view HRTEM images of BiOCl NS-3; (b) side view HRTEM images of BiOCl NS-3; and (c) simulation structure of single BiOCl NS [44]. Reprinted with permission from Royal Society of Chemistry.

BiOCl: Our group synthesized the BiOCl nanosheets with different {001} facets (71–87%) percentage through a molecular precursor ($Bi_n(Tu)_xCl_{3n}$ (Tu = thiourea)) route (**Figure 8**) [44]. With the {001} facets percentage increase, the photocatalytic activity increasing strongly. The electron paramagnetic resonance (EPR) and PL techniques were used to study the reason of the high photoactivity of {001} facets. We firstly observed the EPR signal intensity arising from UV light-induced oxygen vacancy and a new PL signal intensity also increased with {001} facets percentage increasing. It was suggested that 100% oxygen atom density in {001} facets was the

fundamental cause for the UV-induced oxygen vacancies generated in the crystal lattice. And then, high UV light photocatalytic activity of BiOCl appeared.

Recently, atomic thickness BiOCl nanosheets were reported [225, 229, 230]. And the researcher found that the high density of oxygen atoms of exposed {001} facets not only are useful for the cationic dye adsorption but also can improve the photo-induced electrons injected via dye excitation. And these photo-induced electrons were captured by O_2 to create reactive oxygen species, which displayed strong photooxidative ability to remove pollutants.

BiOBr: Wu synthesized BiOBr nanosheets with {001} facets exposure by adjusting solvent and reaction temperature [227]. The VLD photocatalytic efficiency for RhB degradation enhanced with the {001} facets percentage increasing from 83 to 94% of BiOBr. Furthermore, the as-synthesized BiOBr nanosheets exhibited selective VLD photocatalytic activity with RhB is much higher than that MO or MB degradation due to the 100% oxygen terminated atoms of {001} facets.

BiOI: Our group prepared the BiOI single-crystal nanosheets (BiOI SCNs) with highly symmetry and dominant exposed {001} facets (up to 95%) via annealing BiI_3 [60]. The synthesis mechanism with thermal decomposition process of BiI_3 was studied. And it was found that the reactive facets of BiOI were {001} facets. The photocatalytic results showed that BiOI SCNs exhibited higher VLD photocatalytic activity for RhB degradation than irregular BiOI. The improved separation efficiency of photo-induced carriers resulted the {001} facet-dependent photocatalytic activity of BiOI. Recently, our group also synthesized BiOI-001 ultrathin nanosheets for CO_2 reduction [231].

5.2. {010} facet

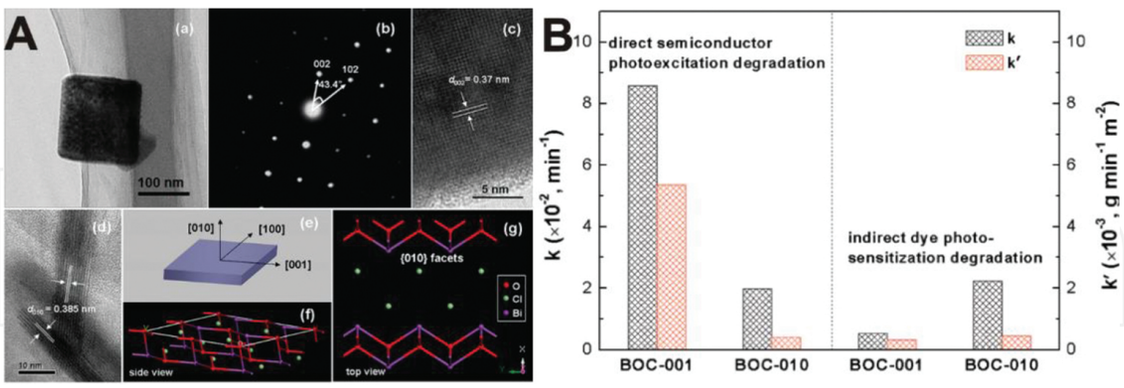

Figure 9 (A): (a) TEM image, (b) SAED pattern, and (c, d) HRTEM images of the BOC-010 SCNSs. (e) Schematic illustration of the crystal orientation of the nanosheet. (f, g) Atomic structure of the {010} facets: (f) side view; (g) top view. (B): Comparison of the apparent reaction rate constants for photocatalytic degradation of MO over the BOC SCNSs under (left) UV (λ = 254 nm) and (right) visible-light (λ > 420 nm) irradiation [210]. Reprinted with permission from American Chemical Society.

BiOCl:In general, the side surface of BiOX nanosheets was {010} facets are and it was difficult to expose due to its high surface energy. So, special synthetic methods should be used to expose {010} facets of BiOX. Recently, Zhang firstly reported the facet controllable synthesis of BiOCl

single-crystalline nanosheets (BOC SCNSs) by adjusting the pH value of the solution with adding NaOH (**Figure 9a**) to exposed {010} or {001} facets [223]. And this method offered to hope to research the facet effect of all BiOX photocatalysts. Based on the surface atomic structure and internal electric fields direction, BiOCl-001 had higher direct photocatalytic activity under UV light. However, BiOCl-010 had superior activity for indirect dye sensitization degradation under visible light due to the open channel characteristic and larger surface area (**Figure 9b**).

BiOBr: Following Zhang's work, Wong also used the same method to synthesize BiOBr single-crystalline nanosheets with {010} facets [70]. The photocatalytic activity results showed the BiOBr-001 exhibited much higher photocatalytic activity for *Escherichia coli* inactivation under visible light. The above same pH controlled method for {010} exposure of BiOCl and BiOBr proved the universality. But, it can be used to exposure {010} facets of BiOI?

BiOI: It was a pity that pH controlled method cannot be used to exposure {010} facets of BiOI. And these results have been proved by many research groups. Fortunately, our group prepared BiOI-010 sample via reaction time method recently [228]. When reaction time was 2 h, the sample was BiOI-010, and BiOI-001 was obtained when the reaction time more than 12 h. The photocatalytic activity data showed BiOI-001 still displayed higher activity than BiOI-010 for CO_2 reduction under UV–Vis light.

5.3. Advice on facets confirmation of BiOX

The basic premise of the facet effect research was the confirming the dominant exposed facet, transmission electron microscope (TEM) images and the corresponding selected-area electron diffraction (SAED) pattern, or high resolution TEM and the corresponding fast-Fourier transform (FFT) pattern were needed. However, the facets confirmation of BiOX was very difficult due to the theoretical value of the angle between the (102) and (002) facets is very close to that of between the (200) and (110) facets. Based on the symmetries of tetragonal BiOX and the above observation, the dominant exposed facets of BiOX samples should be identified discreetly. And our group give some proposals [232].

	a = b (nm)		**110**	**200**	**102**	**002**	
BiOCl	0.3883	0.7347	d value	0.275 nm	0.194 nm	0.267 nm	0.367 nm
			Angle	45.0°		43.4°	
BiOBr	0.3915	0.8076	d value	0.277 nm	0.196 nm	0.281 nm	0.404 nm
			Angle	45.0°		45.9°	
BiOI	0.3984	0.9128	d value	0.282 nm	0.199 nm	0.300 nm	0.456 nm
			Angle	45.0°		48.7°	

Table 1. Theoretical d value of the theoretical angles of relevant diffraction spots.

Table 1 shows the theoretical angles of (110)/(200) and (102)/(200) and the theoretical d value of (110), (200), (102), and (200) of BiOX. We found the theoretical angles of (110)/(200) which very close to that of (102)/(200), especially for BiOBr. But, the theoretical d values of (110), (200), (102), and (200) of BiOX were different. The $d_{(001)}$ of BiOX were much higher than that of (110), (200), and (102). So, if the SAED or FFT pattern had scaleplate, the d values of the diffraction spots can be indexed and the exposed facets can be confirmed.

6. Summary and future perspectives

This chapter summarized the recent studies about BiOX for efficient photocatalytic degradation removal of gas, liquid, and solid pollutants. Firstly, advanced synthesis methods resulted high surface area and {001} facets exposure of BiOX with excellent photocatalytic performances. Secondly, after the modification with cocatalyst using, element doping, semiconductor coupling, dye sensitization, surface plasmon resonance, defect making, bismuth-rich effect BiOX displayed excellent photocatalytic activity for environmental remediation under visible light. At end, we give some proposals to confirm facet exposure for studying facet-dependent photocatalytic properties of BiOX. Although there are many achievements about BiOX photocatalysis, there still many fields were needed to research, such as photocatalytic H_2 generation, photocatalytic CO_2 reduction, photocatalytic N_2 fixation, good synthesis methods for active facets exposure, and more deeply photocatalytic mechanism studies. The corporate efforts of experimental studies and theory computations should be used to resolve the above questions. The unsatisfactory points and future research directions include the following:

(1) In general, BiOX were 2D nanosheets with {001} facets exposing. Other morphologies, such as 1D nanorods and 3D nanocube, and other high index facets exposing were reported few. New synthesis ways should be employed to expose the high index facet of BiOX. In addation, BiOX immobilization should be studied to perfect the practical application.

(2) To date, most reports about BiOX photocatalysts were focused on the PCD of liquid organic pollutants. BiOX photocatalysis in atmospheric and solid-phase contaminants should be enhanced. Furthermore, except for our group, BiOX were rarely used in energy photocatalysis field, such as water splitting and CO_2 photoreduction. It should be expanded the energy photocatalysis field for BiOX.

(3) As the layered crystal structure of BiOX interlacing of $[Bi_2O_2]$ slabs with double halogen slabs, the strong ionic feature could result in ion exchange reactions between BiOX and incoming species. For instances, Bi_2S_3 disk-like networks [233], and Bi_2WO_6 hollow microspheres [234] were prepared by this strategy. It indicated that BiOX had wide applications, not only can be used as photocatalysts but also can be used as hard template to synthesize other photocatalysts with different nanostructures.

Acknowledgements

This work was supported by the National Natural Science Foundation of China (Nos. 51502146, U1404506), Natural Science Foundation of Henan Department of Science & Technology (No. 142102210477), Natural Science Foundation of Henan Department of Education (No. 14A150021), Natural Science Foundation of Nanyang Normal University (No. ZX2014039).

Author details

Liqun Ye

Address all correspondence to: yeliquny@163.com

1 College of Chemistry and Pharmaceutical Engineering, Nanyang Normal University, Nanyang, China

2 School of Oil and Natural Gas Engineering, Southwest Petroleum University, Chengdu, China

References

[1] Chen H., Nanayakkara C. E., Grassian V. H., Chem. Rev., 2012, 112, 5919–5948.

[2] Chen C., Ma W., Zhao J., Chem. Soc. Rev., 2010, 39, 4206–4219.

[3] Konstantinou I. K., Albanis T. A., Appl. Catal. B, 2004, 49, 1–14.

[4] Kubacka A., Fernández-García M., Colón G., Chem. Rev., 2012, 112, 1555–1614.

[5] Wang Y., Wang X., Antonietti M., Angew. Chem. Int. Ed., 2011, 50, 2–24.

[6] Chen X., Shen S., Guo L., Mao S. S., Chem. Rev., 2010, 110, 6503–6570.

[7] Khin M. M., Nair A. S., Babu V. J., Murugan R., Ramakrishna S., Energy. Environ. Sci., 2013, 5, 8075–8109.

[8] Andreozzi R., Caprio V., Ermellino I., Tufano A. I., Ind. Eng. Chem. Res., 1996, 35, 1467–1471.

[9] Linsebigler A. L., Lu G., Yates J. T., Chem. Rev., 1995, 95, 735–758.

[10] Dalrymple O. K., Stefanakos E., Trotz M. A., Goswami D. Y., Appl. Catal. B, 2010, 98, 27–38.

[11] Thompson T. L., Yates J. T., Chem. Rev., 2006, 106, 4428–4453.

[12] Serpone N., Emeline A. V., J. Phys. Chem. Lett., 2012, 3, 673–677.

[13] Hoffmann M. R., Martin S. T., Choi W., Bahnemannt D. W., Chem. Rev., 1995, 95, 69–96.

[14] Linic S., Christopher P., Ingram D. B., Nat. Mater., 2011, 10, 911–921.

[15] Xiang Q., Yu J., Jaroniec M., Chem. Soc. Rev., 2012, 41, 782–796

[16] Liu S., Yu J., Cheng B., Jaroniec M., Adv. Colloid. Interface. Sci., 2012, 173, 35–53.

[17] Reed J., Ceder G., Chem. Rev., 2004, 104, 4513–4534.

[18] Burch R., Chalker S., Loader P., Thomas J. M., Ueda W., Appl. Catal. A, 1992, 82, 77–90.

[19] Kijima N., Matano K., Saito M., Oikawa T., Konishi T., Yasuda H., Sato T., Yoshimura Y., Appl. Catal. A., 2001, 206, 237–244.

[20] Kusainova A. M., Lightfoot P., Zhou W., Stefanovich S. Y., Mosunov A. V., Dolgikh V. A., Chem. Mater., 2001, 13, 4731–4737.

[21] Ye L., Wang L., Xie H., Su Y., Jin X., Zhang C., Energy. Technol., 2015, 3, 1115–1120.

[22] Maile F. J., Pfaff G., Reynders P., Prog. Org. Coat., 2005, 54, 150–163.

[23] Zhang K. L., Liu C. M., Huang F. Q., Zheng C., Wang W. D., Appl. Catal. B., 2006, 68, 125–129.

[24] Huang W., Zhu Q., Comput. Mater. Sci., 2008, 43, 1101–1108.

[25] Zhang H., Liu L., Zhou Z., RSC Adv., 2012, 2, 9224–9229.

[26] Wang W., Yang W., Chen R., Duan X., Tian Y., Zeng D., Shan B., Phys. Chem. Chem. Phys., 2012, 14, 2450–2454.

[27] Zhang X., Fan C., Wang Y., Wang Y., Liang Z., Han P., Comput. Mater. Sci., 2013, 71, 135–145.

[28] Zhao L., Zhang X., Fan C., Liang Z., Han P., Phys. B., 2012, 407, 3364–3370.

[29] Yang C., Deng K., Peng T., Zan L., Chem. Eng. Technol., 2011, 34, 1–8.

[30] Zhao X., Li Z., Chen Y., Shi L., Zhu Y., Mol J.. Catal. A., 2007, 268, 101–106.

[31] Zan L., Fang W., Wang S., Environ. Sci. Technol., 2006, 40, 1681–1685.

[32] Yang C., Gong C., Peng T., Deng K., Zan L., J. Hazard. Mater., 2010, 178, 152–156.

[33] Fa W., Zan L., Gong C., Zhong J., Deng K., Appl. Catal. B., 2008, 79, 216–223.

[34] Huang M. H., Lin P. H., Adv. Funct. Mater., 2012, 22, 14–24.

[35] Tong H., Ouyang S., Bi Y., Umezawa N., Oshikiri M., Ye J., Adv. Mater., 2012, 24, 229–251.

[36] Jiang Z. Y., Kuang Q., Xie Z. X., Zheng L. S., Adv. Funct. Mater., 2010, 20, 3634–3645.

[37] Liu G., Yu J. C., Lu G. Q., Cheng H. M., Chem. Commun., 2011, 47, 6763–6783.

[38] Zhang X., Ai Z., Jia F., Zhang L., J. Phys. Chem. C., 2008, 112, 747–753.

[39] Chang X., Huang J., Cheng C., Sui Q., Sha W., Ji G., Deng S., Yu G., Catal. Commun., 2010, 11, 460–464.

[40] An H., Du Y., Wang T., Wang C., Hao W., Zhang J., Rare. Metals., 2008, 27, 243–250.

[41] Deng Z., Chen D., Peng B., Tang F., Cryst. Growth. Des., 2008, 8, 2995–3003.

[42] Liu Z., Xu W., Fang J., Xu X., Wu S., Zhu X., Chen Z., Appl. Surf. Sci., 2012, 259, 441–447.

[43] Peng S., Li L., Zhu P., Wu Y., Srinivasan M., Mhaisalkar S. G., Ramakrishna S., Yan Q., Chem. Asian J., 2013, 8, 258–268

[44] Ye L., Zan L., Tian L., Peng T., Zhang J., Chem. Commun., 2011, 47, 6951–6953.

[45] Peng H., Chan C. K., Meister S., Zhang X. F., Cui Y., Chem. Mater., 2009, 21, 247–252.

[46] Song J. M., Mao C. J., Niu H. L., Shen Y. H., Zhang S. Y., Cryst Eng Comm., 2010, 12, 3875–3881.

[47] Shao C., Liu Y., Micro. Nano. Lett., 2012, 7, 152–154.

[48] Xiong J., Cheng G., Li G. F., Qin F., Chen R., RSC Adv., 2011, 1, 1542–1552.

[49] Zhang L., Cao X. F., Chen X. T., Xue Z. L., J. Colloid. Interface. Sci., 2011, 354, 630–636.

[50] Zhang D., Wen M., Jiang B., Li G., Yu J. C., J. Hazard. Mater., 2012, 212, 104–111.

[51] Xu J., Meng W., Zhang Y., Li L., Guo C., Appl. Catal. B., 2011, 107, 355–362.

[52] Feng Y., Li L., Li J., Wang J., Liu L., J. Hazard. Mater., 2011, 192, 538–544.

[53] Cheng H., Huang B., Wang Z., Qin X., Zhang X., Dai Y., Chem. Eur. J., 2011, 17, 8039–8043.

[54] Ai Z., Ho W., Lee S., Zhang L., Environ. Sci. Technol., 2009, 43, 4143–4150.

[55] Jiang Z., Yang F., Yang G., Kong L., Jones M. O., Xiao T., Edwards P. P., J. Photochem. Photobiol. A., 2010, 212, 8–13.

[56] Wang Y., Deng K., Zhang L., J. Phys. Chem. C., 2011, 115, 14300–14308.

[57] Xia J., Yin S., Li H., Xu H., Yan Y. G., Zhang Q., Langmuir., 2011, 27(3), 1200–1206.

[58] Li Y., Wang J., Yao H., Dang L., Li Z., J. Mol. Catal. A., 2011, 334, 116–122.

[59] Xiao X., Zhang W. D., J. Mater. Chem., 2010, 20, 5866–5870.

[60] Ye L., Tian L., Peng T., Zan L., J. Mater. Chem., 2011, 21, 12479–12484.

[61] Shang M., Wang W., Zhang L., J. Hazard. Mater., 2009, 167, 803–809.

[62] Li Y., Liu J., Jiang J., Yu J., Dalton Trans., 2011, 40, 6632–6634.

[63] Wu S., Fang J., Hong X., K Hui, Y. Cen, Dalton Trans., 2014, 43, 2611–2619.

[64] Hahn N. T., Hoang S., Self J. L., Mullins C. B., ACS Nano., 2012, 6(9), 7712–7722.

[65] Liu M., Zhang L., Wang K., Zheng Z., Cryst Eng Comm., 2011, 13, 5460–5466.

[66] Liu Z., Fang J., Xu W., Xu X., Wu S., X. Zhu. Mater. Lett., 2012, 88, 82–85.

[67] Deng H., Wang J., Peng Q., Wang X., Li Y., Chem. Eur. J., 2005, 11, 6519–6524.

[68] Pare B., Sarwan B., Jonnalagadda S. B., J. Mol. Struct., 2012, 1001, 196–202.

[69] Huo Y., Zhang J., Miao M., Jin Y., Appl. Catal. B., 2012, 111–112, 334–341.

[70] Wu D., Wang B., Wang W., An T., Li G., Ng T. W., Yip H. Y., Xiong C., Lee H. K., Wong P. K., J. Mater. Chem. A., 2015, 3, 15148–15155.

[71] Fang Y. F., Ma W. H., Huang Y. P., Cheng G. W., Chem. Eur. J., 2013, 19, 3224–3229.

[72] Zhang M., Chen C., Ma W., Zhao J., Angew. Chem. Int. Ed., 2008, 47, 9730–9733.

[73] Zhang M., Wang Q., Chen C., Zang L., Ma W., Zhao J., Angew. Chem., 2009, 121, 6197–6200.

[74] Liu S., Yu J., Jaroniec M., J. Am. Chem. Soc., 2010, 132, 11914–11916.

[75] Xiang Q., Yu J., Jaroniec M., Chem. Commun., 2011, 47, 4532–4534.

[76] Chen F., Liu H., Bagwasi S., Shen X., Zhang J., J. Photochem. Photobiol. A., 2010, 215, 76–80.

[77] Weng S., Chen B., Xie L., Zheng Z., Liu P., J. Mater. Chem. A., 2013, 1, 3068–3075.

[78] Li H., Zhang L., Nanoscale., 2014, 6, 7805–7810.

[79] Li H., Shi J., Zhao K., Zhang L., Nanoscale., 2014, 6, 14168–14173.

[80] Liu H., Cao W., Su Y., Wang Y., Wang X., Appl. Catal. B., 2012, 111–112, 271–279.

[81] Yu C., Yu J. C., Fan C., Wen H., Hu S., Mater. Sci. Eng. B., 2010, 166, 213–219.

[82] Ye L., Liu X., Zhao Q., Xie H., Zan L., J. Mater. Chem. A., 2013, 1, 8978–8983.

[83] Zhang X., Zhang L., J. Phys. Chem. C., 2010, 114, 18198–18206.

[84] Zhang K., Zhang D., Liu J., Ren K., Luo H., Peng Y., Li G., Yu X., Cryst Eng Comm., 2012, 14, 700–707.

[85] Li J., Zhao K., Yu Y., Zhang L., Adv. Funct. Mater., 2015, 25, 2189–2201.

[86] Wang P. Q., Bai Y., Liu J. Y., Fan Z., Hu Y. Q., Micro. Nano. Lett., 2012, 7, 876–879.

[87] Pare B., Sarwan B., Jonnalagadda S. B., Appl. Surf. Sci., 2011, 258, 247–253.

[88] Jiang G., Wang X., Wei Z., Li X., Xi X., Hu R., Tang B., Wang R., Wang S., Wang T., Chen W., J. Mater. Chem. A., 2013, 1, 2406–2410.

[89] Wang R., Jiang G., Wang X., Hu R., Xi X., Bao S., Zhou Y., Tong T., Wang S., Wang T., Chen W., Powder. Technol., 2012, 228, 258–263.

[90] Cheng H., Huang B., Qin X., Zhang X., Dai Y., Chem. Commun., 2012, 48, 97–99.

[91] Cao J., Xu B., Lin H., Luo B., Chen S., Catal. Commun., 2012, 26, 204–208.

[92] Chang X., Yu G., Huang J., Li Z., Zhu S., Yu P., Cheng C., Deng S., Ji G., Catal. Today., 2010, 153, 193–199.

[93] Zhang L., Wang W., Zhou L., Shang M., Sun S., Appl. Catal. B., 2009, 90, 458–462.

[94] Chai S. Y., Kim Y. J., Jung M. H., Chakraborty A. K., Jung D., Lee W. I., J. Catal., 2009, 262, 144–149.

[95] Cao J., Zhou C., Lin H., Xu B., Chen S., Appl. Surf. Sci., 2013, 284, 263–269.

[96] Shamaila S., Khan A., Sajjad L., Chen F., Zhang J., Colloid Interface J.. Sci., 2011, 356, 465–472.

[97] Gao B., Chakraborty A. K., Yang J. M., Lee W. I., Bull. Korean. Chem. Soc., 2010, 31, 1941–1944.

[98] Shenawi-Khalil S., Uvarov V., Menes E., Popov I., Sasson Y., Appl. Catal. A. Gen., 2012, 413–414, 1–9.

[99] Wang Q., Hui J., Li J., Cai Y., Yina S., Wang F., Su B., Appl. Surf. Sci., 2013, 283, 577–583.

[100] Kong L., Jiang Z., Xiao T., Lu L., Jones M. O., Edwards P. P., Chem. Commun., 2011, 47, 5512–5514.

[101] Li Y., Liu Y., Wang J., Uchaker E., Zhang Q., Sun S., Huang Y., Li J., Cao G., J. Mater. Chem. A., 2013, 1, 7949–7956.

[102] Fu J., Tian Y., Chang B., Xi F., Dong X., J. Mater. Chem., 2012, 22, 21159–21166.

[103] Ye L., Liu J., Jiang Z., Peng T., Zan L., Appl. Catal. B, 2013, 142–143, 1–7.

[104] Di J., Xia J., Yin S., Xu H., He M., Li H., Xu L., Jiang Y., RSC Adv., 2013, 3, 19624–19631.

[105] Cheng C., Ni Y., Ma X., Hong J., Mater. Lett., 2012, 79, 273–276.

[106] Kong L., Jiang Z., Lai H. H., Nicholls R. J., Xiao T., Jones M. O., Edwards P. P., J. Catal., 2012, 293, 116–125.

[107] Cao J., Xu B., Lin H., Luo B., Chen S., Dalton. Trans., 2012, 41, 11482–11490.

[108] Cui Z., Si M., Zheng Z., Mi L., Fa W., Jia H., Catal. Commun., 2013, 42, 121–124.

[109] Jiang D., Chen L., Zhu J., Chen M., Shi W., Xie J., Dalton Trans., 2013, 42, 15726–15734.

[110] Hou D., Hu X., Hu P., Zhang W., Zhang M., Huang Y., Nanoscale., 2013, 5, 9764–9772.

[111] Li P., Zhao X., Jia C., Sun H., Sun L., Cheng X., Liu L., Fan W., J. Mater. Chem. A., 2013, 1, 3421–3429.

[112] Cao J., Li X., Lin H., Chen S., Fu X., J. Hazard. Mater., 2012, 239–240, 316–324.

[113] Li H., Cui Y., Hong W., Appl. Surf. Sci., 2013, 264, 581–588.

[114] Cao J., Xu B., Lin H., Chen S., Chem. Eng. J., 2013, 228, 482–488.

[115] Li Y., Wang J., Yao H., Dang L., Li Z., Catal. Commun., 2011, 12, 660–664.

[116] Jiang J., Zhang X., Sun P., Zhang L., J. Phys. Chem. C., 2011, 115, 20555–20564.

[117] Li H., Cui Y. , Hong W., Xu B., Chem. Eng. J., 2013, 228, 1110–1120.

[118] Zhang X., Zhang L., Xie T., Wang D., J. Phys. Chem. C., 2009, 113, 7371–7378.

[119] Dai G., Yu J., Liu G., J. Phys. Chem. C., 2011, 115, 7339–7346.

[120] Cheng H., Huang B., Dai Y., Qin X., Zhang X., Langmuir., 2010, 26(9), 6618–6624.

[121] Chen L., Jiang D., He T., Wu Z., Chen M., Cryst Eng Comm., 2013, 15, 7556–7563.

[122] Cheng H., Wang W., Huang B., Wang Z., Zhan J., Qin X., Zhang X., Dai Y., J. Mater. Chem. A., 2013, 1, 7131–7136.

[123] Lv Y., Liu H., Zhang W., Ran S., Chi F., Yang B., Xia A., J. Environ. Chem. Eng., 2013, 1, 526–533.

[124] Li T. B., Chen G., Zhou C., Shen Z. Y., Jin R. C., Sun J. X., Dalton. Trans., 2011, 40, 6751–6758.

[125] Xiao X., Hao R., Liang M., Zuo X., Nan J., Li L., Zhang W., J. Hazard. Mater., 2012, 233–234, 122–130.

[126] Dong F., Sun Y., Fu M., Wu Z., Lee S. C., J. Hazard. Mater., 2012, 219–220, 26–34.

[127] Cao J., Xu B., Luo B., Lin H., Chen S., Catal. Commun., 2011, 13, 63–68.

[128] Cao J., Xu B., Lin H., Luo B., Chen S., Chem. Eng. J., 2012, 185–186, 91–99.

[129] Zhang J., Xia J., Yin S., Li H., Xu H., He M., Huang L., Zhang Q., Colloids Surf. A., 2013, 420, 89–95.

[130] Reddy K. H., Martha S., Parida K. M., Inorg. Chem., 2013, 52, 6390–6401.

[131] Gao F., Zeng D., Huang Q., Tian S., Xie C., Phys. Chem. Chem. Phys., 2012, 14, 10572–10578.

[132] Tian L., Liu J., Gong C., Ye L., Zan L., J. Nano. Res., 2013, 15(9), 1–11.

[133] Tu X., Luo S., Chen G., Li J., Chem. Eur. J., 2012, 18, 14359–14366.

[134] Ai Z., Ho W., Lee S., J. Phys. Chem. C., 2011, 115(51), 25330–25337.

[135] Liu J. Y., Bai Y., Luo P. Y., Wang P. Q., Catal. Commun., 2013, 42, 58–61.

[136] Zhang X., Chang X., Gondal M. A., Zhang B., Liu Y., Ji G., Appl. Surf. Sci., 2012, 258, 7826–7832.

[137] Lei Y., Wang G., Guo P., Song H., Appl. Surf. Sci., 2013, 279, 374–379.

[138] Xiong W., Zhao Q., Li X., Zhang D., Catal. Commun., 2011, 16, 229–233.

[139] Cheng H., Huang B., Wang P., Wang Z., Lou Z., Wang J., Qin X., Zhang X., Dai Y., Chem. Commun., 2011, 47, 7054–7056.

[140] Yan T., Yan X., Guo R., Zhang W., Li W., You J., Catal. Commun., 2013, 42, 30–34.

[141] Li T., Luo S., Yang L., J. Solid. State. Chem., 2013, 206, 308–316.

[142] Cao J., Zhao Y., Lin H., Xu B., Chen S., J. Solid. State. Chem., 2013, 206, 38–44.

[143] Li T., Luo S., Yang L., Mater. Lett., 2013, 109, 247–252.

[144] Ye L., Liu J., Gong C., Tian L., Peng T., Zan L., ACS Catal., 2012, 2, 1677–1683.

[145] Liu Y., Son W. J., Lu J., Huang B., Dai Y., Whangbo M. H., Chem. Eur. J., 2011, 17, 9342–9349.

[146] Wang W., Huang F., Lin X., Yang J. A., Catal. Commun., 2008, 9, 8–12.

[147] Ren K., Liu J., Liang J., Zhang K., Zheng X., Luo H., Huang Y., Liu P., Yu X., Dalton. Trans., 2013, 42, 9706–9712.

[148] Ye L., Deng K., Xu F., Tian L., Peng T., Zan L., Phys. Chem. Chem. Phys., 2012, 14, 82–85.

[149] Guan M., Xiao C., Zhang J., Fan S., An R., Cheng Q., Xie J., Zhou M., Ye B., Xie Y., J. Am. Chem. Soc., 2013, 135, 10411–10417.

[150] Ye L., Gong C., Liu J., Tian L., Peng T., Deng K., Zan L., J. Mater. Chem., 2012, 22, 8354–8360.

[151] Zhang L., Wang W., Sun S., Sun Y., Gao E., Xu J., Appl. Catal. B., 2013, 132–133, 315–320.

[152] Li R., Zhang F., Wang D., Yang J., Li M., Zhu J., Zhou X., Han H., Li C., Nat. Commun., 2013, 4, 1432.

[153] Jensen R. A., Ryswyk H. V., She C., Szarko J. M., Chen L. X., Hupp J. T., Langmuir., 2010, 26, 1401–1404.

[154] Angelis F. D., Fantacci S., Selloni A., Nazeeruddin M. K., Gratzel M., J. Am. Chem. Soc., 2007, 129, 14156–14157.

[155] Gao F., Wang Y., Shi D., Zhang J., Wang M., Jing X., Humphry-Baker R., Wang P., Zakeeruddin S. M., Gratzel M., J. Am. Chem. Soc., 2008, 130, 10720–10728.

[156] Youngblood W. J., Lee S. A., Maeda K., Mallouk T. E., Acc. Chem. Res., 2009, 42, 1966–1973.

[157] Zhang X., Veikko U., Mao J., Cai P., Peng T., Chem. Eur. J., 2012, 18, 12103–12111.

[158] Pan L., Zou J. J., Zhang X. W., Wang L., J. Am. Chem. Soc., 2011, 133, 10000–10003.

[159] Ji P. F., Zhang J. L., Chen F., Anpo M., Appl. Catal. B, 2009, 85, 148–154.

[160] Chang X., Gondal M. A., Al-Saadi A. A., Ali M. A., Shen H., Zhou Q., Zhang J., Du M., Liu Y., Ji G., J. Colloid. Interface. Sci., 2012, 377, 291–298.

[161] Gondal M. A., Chang X., Ali M. A., Yamani Z. H., Zhou Q., Ji G., Appl. Catal. A., 2011, 397, 192–200.

[162] Zhang L., Wong K. H., Chen Z., Yu J. C., Zhao J., Hu C., Chan C. Y., Wong P. K., Appl. Catal. A., 2009, 363, 221–229.

[163] Zhang Y., Tang Z. R., Fu X., Xu Y. J., Appl. Catal. B., 2011, 106, 445–452.

[164] Wang P., Huang B., Qin X., Zhang X., Dai Y., Wei J., Whangbo M. H., Angew. Chem. Int. Ed., 2008, 47, 7931–7933.

[165] Wang P., Huang B., Lou Z., Zhang X., Qin X., Dai Y., Zheng Z., Wang X., Chem. Eur. J., 2010, 16, 538–544.

[166] Wang P., Huang B., Zhang X., Qin X., Jin H., Dai Y., Wang Z., Wei J., Zhan J., Wang S., Wang J., Whangbo M. H., Chem. Eur. J., 2009, 15, 1821–1824.

[167] An C., Peng S., Sun Y., Adv. Mater., 2010, 22, 2570–2574.

[168] Zhu M., Chen P., Liu M., ACS Nano., 2011, 5, 4529–4536.

[169] Xu H., Li H., Xia J., Yin S., Luo Z., Liu L., Xu L., ACS Appl. Mater. Interfaces., 2011, 3, 22–29.

[170] Li Y., Ding Y., J. Phys. Chem. C., 2010, 114, 3175–3179.

[171] Tian G., Chen Y., Bao H. L., Meng X., Pan K., Zhou W., Tian C., Wang J. Q., Fu H., J. Mater. Chem., 2012, 22, 2081–2088.

[172] Elahifard M. R., Rahimnejad S., Haghighi S., Gholami M. R., J. Am. Chem. Soc., 2007, 129, 9552–9553.

[173] Zhang L. S., Wong K. H., Yip H. Y., Hu C., Yu J. C., Chan C. Y., Wong P. K., Environ. Sci. Technol., 2010, 44, 1392–1398.

[174] Nakamura I., Negishi N., Kutsuna S., Ihara T., Sugihara S., Takeuchi K., J. Mol. Catal. A. Chem., 2000, 161, 205–212.

[175] Ihara T., Miyoshi M., Iriyama Y., Matsumoto O., Sugihara S., Appl. Catal. B., 2003, 42, 403–409.

[176] Chen X., Liu L., Yu P. Y., Mao S. S., Science., 2011, 331, 746–750.

[177] Maeda K., Teramura K., Lu D. L., Takata T., Saito N., Inoue Y., Domen K., Nature., 2006, 440, 295–295.

[178] Wei W., Dai Y., Huang B., J. Phys. Chem. C., 2009, 113, 5658–5663.

[179] Lin X., Huang T., Huang F. Q., Wang W. D., Shi J. L., J. Phys. Chem. B., 2006, 110, 24629–24634.

[180] Li J., Zhang L., Li Y., Yu Y., Nanoscale., 2014, 167–171.

[181] Wang J., Yu Y., Zhang L., Appl. Catal. B., 2013, 136, 112–121.

[182] Xiao X., Xing C. L., He G. P., Zuo X. X., Nan J. M., Wang L. S., Appl. Catal. B., 2014, 148, 154–163.

[183] Di J., Xia J. X., Ji M. X., Yin S., Li H. P., Xu H., Zhang Q., Li H. M., J. Mater. Chem. A., 2015, 3, 15108–15118.

[184] Jin X., Ye L., Wang H., Su Y., Xie H., Zhong Z., Zhang H., Appl. Catal. B. Environ., 2015, 165, 668–675.

[185] Ye L., Jin X., Liu C., Ding C., Xie H., Chu K. H., Wong P. K., Appl. Catal. B Environ., 2016, doi:10.1016/j.apcatb.2016.01.044.

[186] Xiao X., Hu R. P., Liu C., Xing C. L., Zuo X. X., Nan J. M., Wang L. S., Chem. Eng. J., 2013, 225, 790–797.

[187] Xiao X., Hao R., Zuo X. X., Nan J. M., Li L. S., Zhang W. D., Chem. Eng. J., 2012, 209, 293–300.

[188] Sun S. M., Wang W. Z., Zhang L., Zhou L., Yin W. Z., Shang M., Environ. Sci. Technol., 2009, 43, 2005–2010.

[189] Su Y., Wang H., Ye L., Jin X., Xie H., He C., Bao K., RSC Adv., 2014, 4, 65056–65064.

[190] Ye L., Su Y., Jin X., Xie H., Cao F., Guo Z., Appl. Surf. Sci., 2014, 311, 858–863.

[191] Cho S., Jang J. W., Lee J. S., Lee K. H., Langmuir., 2010, 26, 14255–14262.

[192] Fan W., Wang X., Cui M., Zhang D., Zhang Y., Yu T., Guo L., Environ. Sci. Technol., 2012, 46, 10255–10262.

[193] Leng M., Liu M., Zhang Y., Wang Z., Yu C., Yang X., Zhang H., Wang C., J. Am. Chem. Soc., 2010, 132, 17084–17087.

[194] Wang D., Jiang H., Zong X., Xu Q., Ma Y., Li G., Li C., Chem. Eur. J., 2011, 17, 1275–1282.

[195] Wang H., Yang J., Li X., Zhang H., Li J., Guo L., Small., 2012, 8, 2802–2806.

[196] Yi Z., Ye J., Kikugawa N., Kako T., Ouyang S., Stuart-Williams H., Yang H., Cao J., Luo W., Li Z., Liu Y., Withers R. L., Nat. Mater., 2010, 9, 559–564.

[197] Bi Y., Ouyang S., Umezawa N., Cao J., Ye J., J. Am. Chem. Soc., 2011, 133, 6490–6492.

[198] Selloni A., Nat. Mater., 2008, 7, 613–615.

[199] Yang H. G., Sun C. H., Qiao S. Z., Zou J., Liu G., Smith S. C., Cheng H. M., Lu G. Q., Nature., 2008, 453, 638–641.

[200] Yang H. G., Liu G., Qiao S. Z., Sun C. H., Jin Y. G., Smith S. C., Zou J., Cheng H. M., Lu G. Q., J. Am. Chem. Soc., 2009, 131, 4078–4083.

[201] Han X., Kuang Q., Jin M., Xie Z., Zheng L., J. Am. Chem. Soc., 2009, 131, 3152–3153.

[202] Pan J., Liu G., Lu G. Q., Cheng H. M., Angew. Chem. Int. Ed., 2011, 50, 2133–2137.

[203] Zhao X., Jin W., Cai J., Ye J., Li Z., Ma Y., Xie J., Qi L., Adv. Funct. Mater., 2011, 21, 3554–3563.

[204] Wu X., Chen Z., Lu G. Q., Wang L., Adv. Funct. Mater., 2011, 21, 4167–4172.

[205] Yu H., Tian B., Zhang J., Chem. Eur. J., 2011, 17, 5499–5502.

[206] Ye L., Liu J., Jiang Z., Peng T., Zan L., Nanoscale., 2013, 5, 9391–9396.

[207] Ye L., Liu J., Tian L., Peng T., Zan L., Appl. Catal. B, 2013, 134–135, 60–65.

[208] Gordon T. R., Cargnello M., Paik T., Mangolini F., Weber R. T., Fornasiero P., Murray C. B., J. Am. Chem. Soc., 2012, 134, 6751–6761.

[209] Murakami N., Kurihara Y., Tsubota T., Ohno T., J. Phys. Chem. C., 2009, 113, 3062–3069.

[210] Ohno T., Sarukawa K., Matsumura M., New. J. Chem., 2002, 26, 1167–1170.

[211] Tachikawa T., Yamashita S., Majima T., J. Am. Chem. Soc., 2011, 133, 7197–7204.

[212] Tachikawa T., Wang N., Yamashita S., Cui S., Majima T., Angew. Chem., 2010, 122, 8775–8779.

[213] Maitani M. M., Tanaka K., Mochizuki D., Wada Y., J. Phys. Chem. Lett., 2011, 2, 2655–2659.

[214] Arienzo M. D., Carbajo J., Bahamonde A., Crippa M., Polizzi S., Scotti R., Wahba L., Morazzoni F., J. Am. Chem. Soc., 2011, 133, 17652–17661.

[215] Zheng Z., Huang B., Lu J., Qin X., Zhang X., Dai Y., Chem. Eur. J., 2011, 17, 15032–15038.

[216] Xiang Q., Lv K., Yu J., Appl. Catal. B, 2010, 96, 557–564.

[217] Ye L., Mao J., Liu J., Jiang Z., Peng T., Zan L., J. Mater. Chem. A., 2013, 1, 10532–10537.

[218] Han X. G., He H. Z., Kuang Q., Zhou X., Zhang X. H., Xu T., Xie Z. X., Zheng L. S., J. Phys. Chem. C., 2009, 113, 584–589.

[219] Zheng Z., Huang B., Wang Z., Guo M., Qin X., Zhang X., Wang P., Dai Y., J. Phys. Chem. C., 2009, 113, 14448–14453.

[220] Zhang Y., Deng B., Zhang T., Gao D., Xu A. W., J. Phys. Chem. C., 2010, 114, 5073–5079.

[221] Huang W. C., Lyu L. M., Yang Y. C., Huang M. H., J. Am. Chem. Soc., 2012, 134, 1261–1267.

[222] Wang J., Teng F., Chen M., Xu J., Song Y., Zhou X., Cryst Eng Comm., 2013, 15, 39–42.

[223] Jiang J., Zhao K., Xiao X., Zhang L., J. Am. Chem. Soc., 2012, 134, 4473–4476.

[224] Ye L., Chen J., Liu J., Peng T., Deng K., Zan L., Appl. Catal. B, 2013, 130–131, 1–7.

[225] Wang D. H., Gao G. Q., Zhang Y. W., Zhou L. S., Xu A. W., Chen W., Nanoscale., 2012, 4, 7780–7785.

[226] Wang C., Zhang X., Yuan B., Shao C., Liu Y., Micro. Nano. Lett., 2012, 7, 152–154.

[227] Zhang D., Li J., Wang Q., Wu Q., J. Mater. Chem. A., 2013, 1, 8622–8629.

[228] Ye L., Jin X., Ji X., Liu C., Su Y., Xie H., Liu C., Chem. Eng. J., 2016, 291, 39–46.

[229] Ye L., Jin X., Leng Y., Su Y., Xie H., Liu C., J. Power. Sources., 2015, 293, 409–415.

[230] Guan M., Xiao C., Zhang J., Fan S., An R., Cheng Q., Xie J., Zhou M., Ye B., Xie Y., Am J.. Chem. Soc., 2013, 135(28), 10411–10417.

[231] Ye L., Wang H., Jin X., Su Y., Wang D., Xie H., Liu X., Liu X., Sol. Energy. Mater. Sol. C., 2016, 144, 732–739.

[232] Ye L., Su Y., Jin X., Xie H., Zhang C., Environ. Sci. Nano, 2014, 1, 90–112.

[233] Chen J. I. L., von Freymann G., Kitaev V., Ozin G. A., J. Am. Chem. Soc., 2007, 129, 1196–1202.

[234] Cheng H. F., Huang B. B., Liu Y. Y., Wang Z. Y., Qin X. Y., Zhang X. Y., Dai Y., Chem. Commun., 2012, 48, 9729–9731.

IntechOpen